JOURNAL OF VIROLOGY, July 2008, p. 6288–6298 Vol. 82, No. 13
0022-538X/08/$08.00+0 doi:10.1128/JVI.00569-08
Copyright © 2008, American Society for Microbiology. All Rights Reserved.

Bovine Papillomavirus Type 1: from Clathrin to Caveolin▽

Valerie Laniosz,[1] Kirsten A. Holthusen,[2] and Patricio I. Meneses[1,2]*

School of Graduate and Postdoctoral Studies, Department of Microbiology and Immunology, H. M. Bligh Cancer Research Laboratory,[1] and Chicago Medical School,[2] Rosalind Franklin University of Medicine and Science, North Chicago, Illinois 60064

Received 13 March 2008/Accepted 10 April 2008

Viruses may infect cells through clathrin-dependent, caveolin-dependent, or clathrin- and caveolin-independent endocytosis. Bovine papillomavirus type 1 (BPV1) entry into cells has been shown to occur by clathrin-dependent endocytosis, a pathway that involves the formation of clathrin-coated pits and fusion to early endosomes. Recently, it has been demonstrated that the closely related JC virus can enter cells in clathrin-coated vesicles and subsequently traffic to caveolae, the organelle where vesicles of the caveolin-dependent pathway deliver their cargo. In this study, we use immunofluorescence staining of BPV1 pseudovirions to show that BPV1 overlaps with the endosome marker EEA1 early during infection and later colocalizes with caveolin-1. We provide evidence through the colocalization of BPV1 with transferrin and cholera toxin B that BPVl trafficking may not be restricted to the clathrin-dependent pathway. Disrupting the entry of caveolar vesicles did not affect BPV1 infection; however, we show that blocking the caveolar pathway postentry results in a loss of BPV1 infection. These data indicate that BPV1 may enter by clathrin-mediated endocytosis and then utilize the caveolar pathway for infection, a pattern of trafficking that may explain the slow kinetics of BPV1 infection.

Papillomaviruses (PVs) are nonenveloped double-stranded DNA viruses with an 8-kb circular genome. These viruses infect the basal, undifferentiated cells of the squamous epithelia and require host cell factors to replicate (41). PVs are responsible for causing disease in both animals and humans, infecting 6.2 million individuals in the United States each year (www.cdc.gov). Infection with one of the 13 high-risk oncogenic human PVs has been linked to cancers of the cervix, anus, mouth, skin, larynx, penis, and vulva (2, 3, 9, 13–15). Bovine PV (BPV) has served as an excellent model for the study of human PVs, and since BPV infection causes substantial morbidity in cattle, its study is merited (8). The current understanding of how these viruses enter and traffic through the cell has not been fully elucidated, and many discrepancies remain. The major capsid protein, L1, is responsible for the primary binding to the keratinocyte surface (24, 34). While a common cellular receptor has not been identified, two have been suggested: heparan sulfate (35) and the α6β4 integrin complex (16). The existing model of viral internalization supports the clathrin-mediated entry of BPV type 1 (BPV1), human PV type 16 (HPV16), and HPV58, despite a half-life of entry of 4 h (5, 12) and the observed neutralization of PV infection up to 24 h postattachment (10). The kinetics of particle entry by clathrin-mediated endocytosis are usually much faster, ranging from 5 to 15 min (17). Ligands taken up by clathrin-mediated endocytosis are internalized in clathrin-coated vesicles, which normally fuse to early endosomes and are sorted to either the late endosome/lysosome or the recycling endosome for transport back to the plasma membrane (37). HPV31 has been found by some investigators to utilize caveola-dependent endocytosis (5, 39), a pathway which involves the invagination of the plasma membrane at caveolin-stabilized lipid rafts and subsequent fusion with larger cholesterol-rich caveosomes (28). Another study recently demonstrated that HPV31 enters both human and monkey cells in a clathrin-mediated manner, with no reliance on the caveolar pathway (20). The ambiguity in the literature on PV entry suggests that viral entry is a complex process.

A naked double-stranded DNA virus similar in structure to PV and previously grouped in the same family, JC virus (JCV), was shown to enter cells by clathrin-mediated endocytosis and then be escorted to a caveosome prior to delivery to the endoplasmic reticulum (ER) (32). It had been presumed that JCV trafficked solely via the clathrin-dependent pathway since viral entry was blocked by inhibitors of clathrin-dependent endocytosis and dominant negative Eps15 (30). Despite requiring caveolin-1 for infection, JCV infection was shown to be unaffected by chemical inhibitors of caveolar endocytosis, and the virus colocalized with transferrin (Tfn) at 20 min postinternalization (31). The transit of JCV from endosomes to caveosomes provides evidence that viruses can take advantage of the cross talk that occurs between cellular vesicles of different pathways.

It appears that a lack of strict dependence on one pathway is an emerging theme in viral entry. Influenza virus, once thought to enter cells only by the clathrin-dependent pathway, was found to have an alternate means of entry (38). Blocking both the clathrin-dependent and caveolar pathways still resulted in infection, indicating that the virus could enter cells by an unknown route (38). The nonenveloped simian virus 40 (SV40) is noteworthy as one of the few viruses to utilize the caveola-dependent pathway of entry (29). Interestingly, SV40-activated endocytosis from the plasma membrane to the ER was demonstrated in a pathway not involving caveolin or clathrin (11). Another nonenveloped virus previously thought to enter by the clathrin-dependent pathway, poliovirus, has now been shown to enter by a mechanism that is tyrosine kinase and actin

* Corresponding author. Mailing address: Department of Microbiology and Immunology, Rosalind Franklin University of Medicine and Science, 3333 Green Bay Road, 2.351, North Chicago, IL 60064. Phone: (847) 578-3000, ext. 7775. Fax: (847) 578-3349. E-mail: patricio.meneses@rosalindfranklin.edu.

▽ Published ahead of print on 16 April 2008.

dependent. The pathway for poliovirus entry is clathrin, caveolin, flotillin, and microtubule independent (6).

Our laboratory identified BPV1 pseudovirions (PsVs) in the ER using transmission electron microscopy, and immunofluorescence studies showed colocalization between BPV1 and the ER marker calnexin (4, 22). We characterized the interaction between the ER-resident protein syntaxin 18 and the BPV1 minor capsid protein L2, an interaction necessary for infection (22). Cells transfected with FLAG-tagged dominant negative syntaxin 18 prior to BPV1 infection were incapable of supporting a productive viral infection (4). The required interaction of BPV1 with the ER-resident protein syntaxin 18 for infection seemed to indicate that the observed viral particles in the ER were indeed part of the infectious pathway. The clathrin-dependent pathway, currently the accepted model of BPV1 entry, does not typically lead to the ER (27, 28, 37).

A high particle-to-infectivity ratio has complicated studies of the infectious pathway of both PVs and polyomaviruses. Using polyomavirus-like particles encapsidating reporter DNA, investigators previously found two pathways for viral trafficking, one leading to the efficient delivery of the pseudogenome and the other along a noninfectious route (21). Our laboratory has described the internalization and trafficking of noninfectious mutant PsVs, which appear to traffic identically to wild-type (WT) PsVs until about 4 h postinternalization, when the WT virions arrive at the syntaxin 18-positive region of the cell and the mutant virions appear to be retained in the lysosomes (22). Indeed, it has been shown that for roughly every 2,000 wart-derived BPV1 virions, only 1 viral particle is infectious (33). It is difficult to differentiate between viruses that will lead to productive infection and those that will not, making dominant negative proteins and short hairpin RNAs (shRNAs) that block trafficking at specific points an especially useful tool for identifying the infectious pathway of a virus.

In this paper, we used inhibitors of endocytosis, dominant negative caveolin-1, shRNA against caveolin-1, and a caveolin-1 scaffolding mutant (SM) to determine whether caveolin-1 was mediating the entry and trafficking of BPV1. We demonstrate that BPV1 is fully capable of infecting cells without cholesterol and caveolin-1 at the plasma membrane, but we show a nearly complete loss of infection when caveolin-1 expression is knocked down. This finding was of particular interest since BPV1 dependence on clathrin-mediated endocytosis has been well documented (12, 39). Our studies provide further evidence of the existence of cross talk between different types of endocytosis.

MATERIALS AND METHODS

Reagents. shRNA A and B against caveolin-1 and WT and SM Myc–caveolin-1 were a generous gift from W. J. Atwood and W. Querbes (Brown University, Providence, RI). Dominant negative green fluorescent protein (GFP)–caveolin-1 was kindly provided by A. Helenius (Swiss Federal Institute of Technology, Zurich, Switzerland). The pCSC-SP-PW lentiviral vector was generously given by V. Bottero (Rosalind Franklin University of Medicine and Science, North Chicago, IL). BPV1 PsVs were generated and titers were determined as described previously (7) (http://home.ccr.cancer.gov/lco/default.asp). The 293TT cell line, bicistronic BPV1 L1 and L2 plasmid pShell, and GFP cDNA containing plasmid 8fwb or DsRed reporter 8frb used in their production were a gift from P. Day and J. Schiller (NCI, NIH, Bethesda, MD).

Western blot analysis. 293 cells were transfected using GeneJet according to the manufacturer's instructions (SignaGen Laboratories, Gaithersburg, MD). Forty-eight hours posttransfection, cells were harvested in cold 0.5% NP-40 buffer (150 mM NaCl, 5 mM EDTA, 10 mM Tris [pH 7.5]) containing protease inhibitors (GE Healthcare, Piscataway, NJ). Samples were run on a 12% sodium dodecyl sulfate-polyacrylamide gel as described previously (4). The following primary antibodies were used: mouse anti-caveolin-1 (Abcam, Cambridge, MA) and mouse anti-actin (Sigma, St. Louis, MO) were used at a 1:1,000 dilution overnight at 4°C. The anti-Myc hybridoma 9E10 was used at a 1:10 dilution (a gift from E. Robertson, University of Pennsylvania, Philadelphia, PA). Alexa Fluor 680-nm and 800-nm anti-mouse secondary antibodies were used at a 1:20,000 dilution for 30 min at room temperature (Invitrogen, Carlsbad, CA). Blots were scanned using an Odyssey imaging system and viewed using Odyssey-provided software (Li-Cor Inc., Lincoln, NE).

Immunofluorescence. 293 cells were grown on glass coverslips (catalog number 12-545-80; Fisher Scientific, Piscataway, NJ) prior to transfection with 3 μg of dominant negative GFP–caveolin-1, enhanced GFP (EGFP), shRNA A, WT Myc–caveolin-1, or SM Myc–caveolin-1. Coverslips were treated as described previously (4). The following primary antibodies were used at a working dilution of 1:100: mouse anti-L1 hybridoma 5B6, which binds L1 in the intact viral capsid or L1 pentamers (a gift from R. B. Roden, John Hopkins University, Baltimore, MD); the early endosome marker goat anti-EEA1 (Santa Cruz, Santa Cruz, CA); and the caveolar marker rabbit anti-caveolin-1 (Cell Signaling Technology, Danvers, MA). The 647-conjugated anti-Myc antibody was used at a 1:100 dilution (Cell Signaling Technology). Donkey anti-mouse 488, donkey anti-mouse 594, chicken anti-goat 488, donkey anti-rabbit 488, and donkey anti-rabbit 594 fluorescent Alexa Fluor secondary antibodies were used at a 1:2,000 dilution, and donkey anti-rabbit 647 secondary antibody was used at a 1:1,000 dilution (Invitrogen). TOPRO-3 was used for nuclear visualization at a 1:1,000 dilution in the secondary antibody dilution (Invitrogen). All dilutions were made using blocking buffer (0.2% fish skin gelatin, 0.2% Triton X-100, phosphate-buffered saline [PBS]) except that when studies involved the Tfn, the blocking buffer was made using BD Perm/Wash buffer (BD Biosciences, San Jose, CA) and 0.2% fish skin gelatin. Coverslips were mounted using ProLong Gold Antifade (Invitrogen). An Olympus Fluoview 300 fluorescent confocal microscope at the microscopy core of Rosalind Franklin University of Medicine and Science was used for data collection, and analysis was performed using Fluoview software (Olympus, Melville, NY). *z*-stacked images represent a 0.5-μm section of the cell in the *x*, *y*, and *z* planes.

Tfn and CTB internalization. The fluorescently labeled Alexa Fluor 594-Tfn and 594-cholera toxin B (CTB) conjugates were obtained from Invitrogen. In studies involving Tfn, 10 μg/ml of the conjugate was added to chilled 293 cells grown on glass coverslips for 2 h on ice. The cells were then warmed to 37°C at the indicated time points and acid treated to remove unbound Tfn as described previously by Sharma et al. (36). CTB trafficking was studied by the addition of cholera toxin at 1 μg/ml to 293 cells grown on coverslips for 15 min on ice. Cells were transferred into a 37°C incubator for the indicated times, washed in PBS, incubated with anti-cholera toxin antibody for 10 min at 4°C, and washed again prior to fixation. To study the coincident internalization of Tfn and BPV1, both ligands were incubated with the cells on ice for 2 h prior to the shift to 37°C. For the experiment involving the trafficking of BPV1 and CTB, BPV1 was added to chilled cells and incubated on ice for 2 h, and cholera toxin was added during the last 15 min of incubation.

Infection of cells expressing GFP–dominant negative caveolin-1, EGFP, shRNA against caveolin-1, or siRNA control against luciferase. Two hundred thousand 293 cells were transfected with 2 μg of the indicated construct or infected with the luciferase control silencing RNA (siRNA) in the pCSC-SP-PW lentiviral vector. After 48 h, when expression was determined to be stable, cells were chilled on ice prior to the addition of BPV1 PsVs containing a DsRed reporter plasmid. BPV1 was incubated on ice with transfected and untransfected cells for 2 h. Cells were then gently washed with medium to remove unbound virus and warmed to 37°C for 48 h. Cells were then harvested with trypsin and washed with PBS. An LSRII flow cytometer and FACS Diva software (BD Biosciences) were used to detect the percentage of GFP-expressing cells that were also DsRed positive.

Infection of 293 cells transfected with WT Myc-tagged caveolin-1 or the SM. Cells were transfected with 2 μg of DNA and infected with BPV1 PsVs containing the GFP reporter gene after 48 h. Cells were harvested for analysis using a FACSCalibur flow cytometer and CellQuest Pro software (BD Biosciences).

Endocytosis inhibitors. Inhibitors were used at the following concentrations: 1.5 μM filipin (Sigma) and 14 μM chlorpromazine (Sigma). Inhibitors were preincubated with cells at 37°C for 1 h prior to the addition of virions, Tfn, or cholera toxin. The inhibitor was present throughout the infection/ligand internalization.

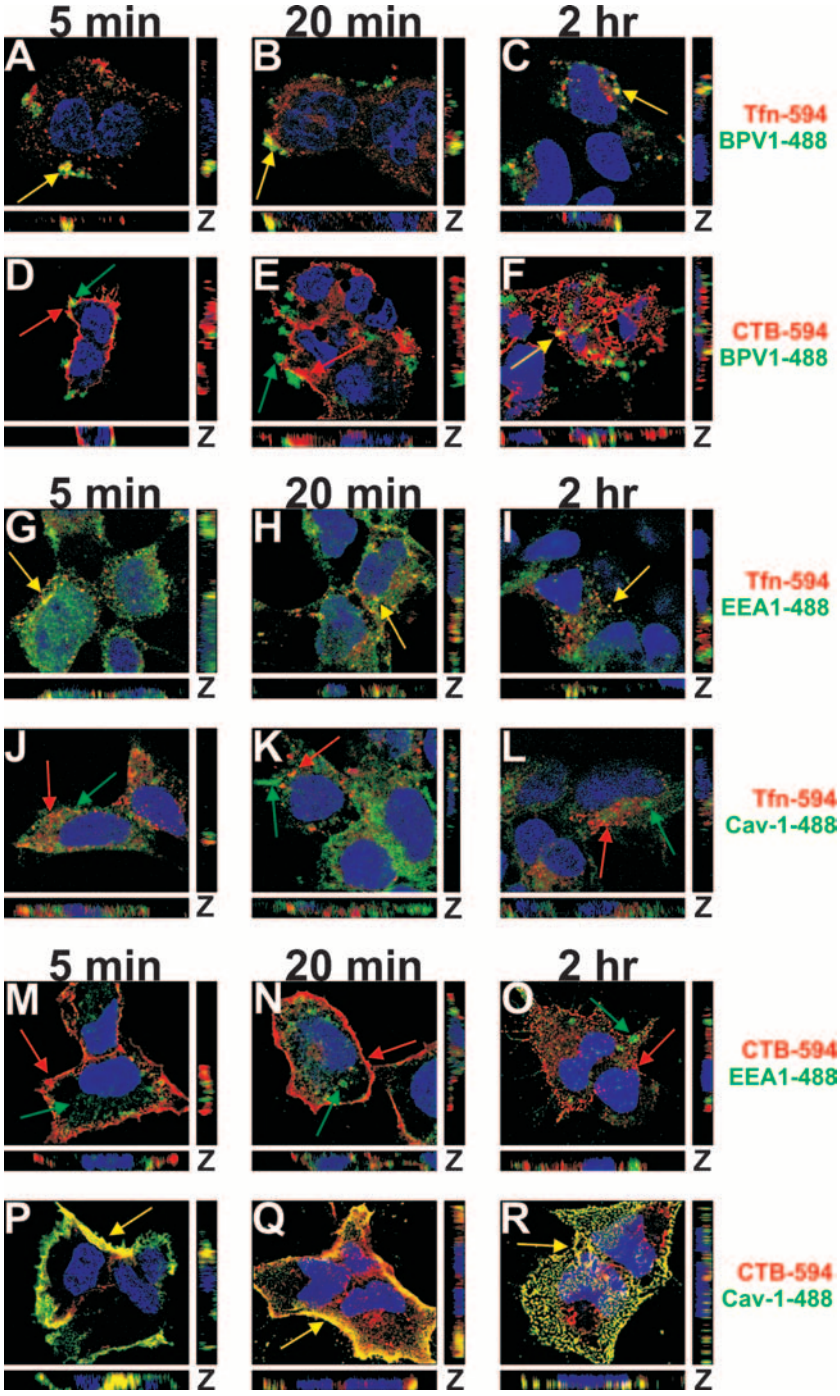

FIG. 1. BPV1 PsVs colocalize with Tfn early during infection and later show overlap with CTB. (A to F) BPV1 PsVs were internalized into 293 cells simultaneously with 594-labeled Tfn (A to C, red) or CTB (D to F, red). Virions were labeled with anti-L1 antibody 5B6 (green), and TOPRO-3 was used to stain the nucleus (blue). At 5 and 20 min, the virus overlapped with Tfn (A and B, yellow) but not CTB (D and E). Two hours postinternalization, there was prominent overlap between BPV1 and CTB (F, yellow) and residual overlap with Tfn (C). (G to L) 293 cells were allowed to internalize Tfn (red) for 5 min, 20 min, and 2 h and stained for the early endosome marker EEA1 (G to I, green) and caveolin-1 (Cav-1) (J to L, green). Tfn colocalized with EEA1 at all time points (G to I, yellow). No overlap was seen between Tfn and caveolin-1 at any of the time points (J to L). (M to R) 293 cells internalized CTB (red) for 5 min, 20 min, and 2 h. EEA1 (M to O, green) and caveolin-1 (P to R, green) were labeled in the cells. Colocalization was observed between CTB and caveolin-1 at all time points (P to R, yellow) but not between CTB and EEA1 (M to O). Images shown are *z* stacks, representing the cell in the *x*, *y*, and *z* planes.

RESULTS

BPV1 trafficking intersects the movement of Tfn and CTB within 293 cells. Although BPV1 entry was previously described to enter via the clathrin-dependent pathway (12), the kinetics of BPV1 infection suggest that the virions may traffic in a non-clathrin-mediated manner. In order to explore this possibility, we wanted to correlate the viral trafficking with known ligands of clathrin- and caveolin-dependent endocyto-

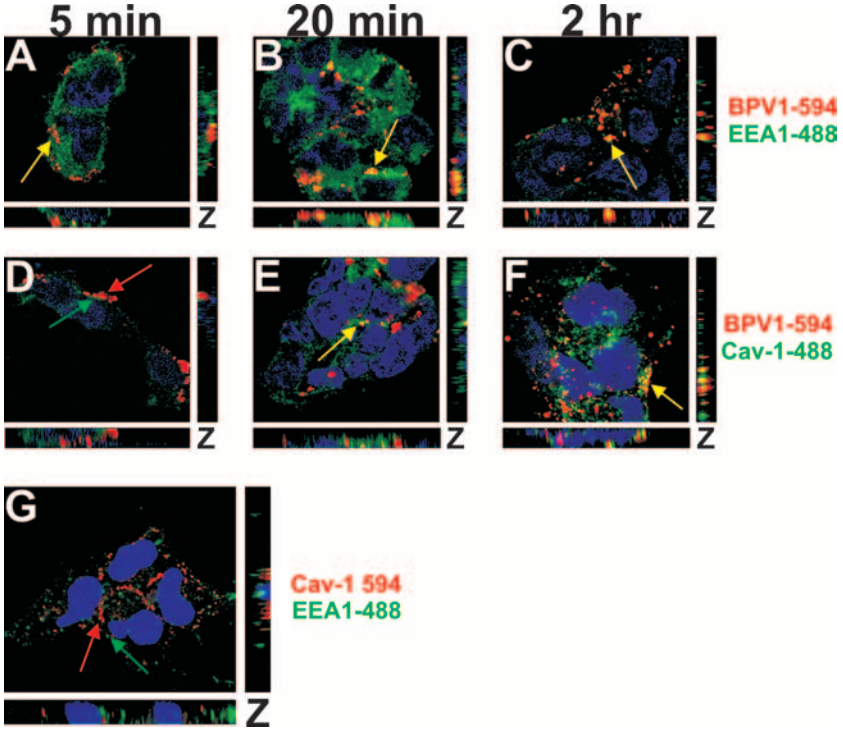

FIG. 2. BPV1 PsVs colocalize with caveolin-1 by 2 h after entry. (A to F) 293 cells were infected with BPV1 PsVs for 5 min, 20 min, and 2 h. Monoclonal antibody 5B6 was used to detect BPV1 (red), the cells were stained for EEA1 (A to C, green) or caveolin-1 (Cav-1) (D to F, green), and the nucleus was stained blue. Five minutes after entry, BPV1 overlapped with EEA1 (A, yellow) but not caveolin-1 (D). At 20 min, colocalization was seen between BPV1 and EEA1 (B, yellow) and to a lesser extent between BPV1 and caveolin-1 (E). Two hours postentry, 5B6 overlapped with EEA1 (C, yellow) and prominently with caveolin-1 (F, yellow). (G) 293 cells were fixed and costained for caveolin-1 (red), EEA1 (green), and nuclei (blue) (TOPRO-3). The markers did not overlap (red and green arrows). Pictures are three-dimensional *z* stacks.

sis, Tfn and CTB, respectively (18, 19, 25). After the coincident internalization of BPV1 and Alexa Fluor 594-labeled Tfn (Fig. 1, red) or CTB (red), the cells were fixed at 5 min, 20 min, and 2 h; BPV1 L1 was detected using 5B6 (Fig. 1, green), and the nucleus was visualized with TOPRO-3 (blue). At 5 min, BPV1 and Tfn demonstrated a considerable amount of colocalization (Fig. 1A, yellow). The overlap between BPV1 and Tfn was most striking at 5 and 20 min after entry (Fig. 1A and B, yellow) and decreased by 2 h (Fig. 1C, yellow). In cells that internalized CTB along with the virus, no significant overlap was seen between CTB and the BPV1 PsVs at 5 and 20 min (Fig. 1D and E). Unexpectedly, there was a substantial amount of overlap between CTB and BPV1 at 2 h (Fig. 1F, yellow). The colocalization of BPV1 (5B6) and Tfn was observed in approximately 75% of cells at 5 min and 20 min and in 50% of the cells at 2 h; the colocalization of BPV1 (5B6) and CTB was observed in less than 10% of cells at 5 min and 20 min and in more than 50% of the cells at 2 h.

To understand the significance of the colocalization between the virions and the clathrin- and caveolin-dependent ligands, we needed to confirm that Tfn and CTB were indeed trafficking by the expected mechanisms. Tfn was internalized by 293 cells, and immunofluorescence was performed in order to explore the receptor location at 5 min, 20 min, and 2 h. We first stained for the early endosome marker EEA1 (Fig. 1G to I, green) since Tfn is known to utilize the early endosome for its entry. A modest amount of colocalization was seen between Tfn and the early endosome (Fig. 1G to I, yellow). An antibody against caveolin-1 (Fig. 1J to L, green) was used to detect caveolar vesicles and the caveosome, vesicles involved in the clathrin-independent mechanism of endocytosis. No colocalization between Tfn and caveolin-1 was seen at any of the time points (Fig. 1J to L).

To confirm that CTB was trafficking by the caveolar pathway, we performed immunofluorescence with CTB (red) and EEA1 (green) (Fig. 1M to O) to determine whether CTB was interacting with the early endosome. The lack of colocalization of CTB with EEA1 confirmed that CTB did not traffic to the early endosome, a vesicle involved in the clathrin-mediated pathway (Fig. 1M to O). Costaining for caveolin-1 (green) and CTB revealed near-complete colocalization (Fig. 1P to R, yellow).

In these experiments, the colocalization between Tfn and the virus or CTB and the virus suggests that BPV1 PsVs are interacting with vesicles of both clathrin- and caveolin-mediated endocytosis.

BPV1 PsVs overlap with the early endosome marker EEA1 early during infection and later colocalize with caveolin-1. To expand on the importance of the observed colocalization between CTB and BPV1, we analyzed the interaction between BPV1 and the early endosome marker EEA1 (Fig. 2A to C, green) and BPV1 and caveolin-1 (Fig. 2D to F, green). The PsVs were detected using monoclonal antibody 5B6 against L1 (Fig. 2A to F, red). A slight interaction was observed between

BPV1 PsVs and EEA1 at 5 min (Fig. 2A, yellow), the greatest overlap was seen at 20 min (Fig. 2B, yellow), and the overlap was diminished by 2 h (Fig. 2C, yellow). As with the staining of BPV1 and CTB, we observed little to no overlap in fluorescence between BPV1 PsVs and caveolin-1 at 5 min (Fig. 2D) and 20 min (Fig. 2E) and an increase in overlapping signals at 2 h (Fig. 2F, yellow). To determine whether there was overlap between EEA1 and caveolin-1 in 293 cells (Fig. 2B), we costained cells for EEA1 (Fig. 2G, green) and caveolin-1 (Fig. 2G, red) and did not identify colocalization between the two vesicular markers. These immunofluorescence studies hint that the caveolar pathway is involved in the trafficking of BPV1 PsVs.

BPV1 does not use the caveolar pathway as an alternate means of entry in 293 cells. The colocalization between BPV1 and both CTB, a caveolar ligand, and caveolin-1 led us to hypothesize that caveolin-mediated endocytosis may be playing a role during infection. To determine if the caveolar pathway was a necessary part of the infectious pathway for BPV1, we decided to block caveolin- and clathrin-mediated internalization. In an effort to prevent viral entry, we used specific biochemical inhibitors of endocytosis: filipin, a drug which sequesters cholesterol from lipid rafts and is known to inhibit caveolin-mediated endocytosis (12, 25, 39), and chlorpromazine, a drug which prevents the assembly of clathrin-coated pits (12, 30, 40). We first wanted to confirm that the concentration of inhibitors added to cells would be nontoxic but still block the entry of cargo known to traffic by these endocytic pathways. 293 cells were preincubated with inhibitors prior to the addition of 594-labeled Tfn or CTB. Thirty minutes after ligand internalization in the presence or absence of the inhibitors, immunofluorescence was performed. Cells that were incubated with Tfn were stained for the early endosome marker EEA1 (Fig. 3A to C, green), cells which were incubated with CTB were stained for caveolin-1 (Fig. 3D to F, green), and the nucleus was stained blue. In untreated cells, Tfn and CTB were evident (Fig. 3A and D, respectively, red), and the ligands colocalized with the markers of their respective endocytic pathways (Fig. 3A and D, yellow). In cells treated with chlorpromazine, the internalization of Tfn was lost (Fig. 3B), while CTB entry was unaffected and colocalized with caveolin-1 (Fig. 3E, yellow). When cells were treated with filipin, there was no change in Tfn detection, and it still overlapped with EEA1 (Fig. 3C, yellow). Caveolin-mediated endocytosis was almost completely blocked, as seen by a loss of CTB entry (Fig. 3F) compared to untreated cells.

After confirming the effectiveness of inhibitor treatment by immunofluorescence, we wanted to explore whether infection with BPV1 PsVs would confirm the literature showing that BPV1 entry is a strictly clathrin-dependent event (12, 39). 293 cells were pretreated with filipin or chlorpromazine, infected with BPV1 PsVs containing a GFP reporter plasmid, and harvested after 48 h to determine the percentage of cells infected by analyzing the percentage of GFP expression (i.e., infection) by flow cytometry. Infection was unaffected by the addition of filipin (5.53% versus 4.92%) (Fig. 3G, bars 1 and 3, respectively) but decreased with chlorpromazine treatment (1.53%) (bar 2). When filipin and chlorpromazine were added together, the decrease in infection did not exceed that with chlorpromazine alone (2.67%) (bar 4), which confirmed that caveolin-mediated entry was not involved in the residual infection observed in chlorpromazine-treated 293 cells.

After verifying that the caveolar pathway was not playing a role in the initial entry of BPV1, we wanted to determine if caveolin-1 was being utilized at a later step in viral trafficking. To study this possibility, 293 cells grown on coverslips were transfected with either an EGFP control (Fig. 3I, green) or dominant negative GFP-tagged caveolin-1 (Fig. 3I, green), which was previously shown to prevent the caveola-mediated uptake of SV40 and HPV31 (29, 39). CTB (Fig. 3, red) was added to transfected cells and internalized for 30 min, and cells were stained for endogenous caveolin-1 (blue). Transfection with dominant negative GFP-tagged caveolin-1 resulted in a nearly total loss of CTB binding/internalization, and ligand-induced movement of endogenous caveolin-1 to the plasma membrane was not observed (Fig. 3H, note the lack of blue in the transfected cell). An untransfected neighboring cell demonstrated the overlap between endogenous caveolin-1 and CTB (Fig. 3H, purple arrow). EGFP expression had no effect on the movement of CTB, and strong colocalization was seen between CTB and endogenous caveolin-1 (Fig. 3I, purple arrow).

In order to determine the effect of dominant negative caveolin-1 expression on BPV1 infection, 293 cells were transfected with either dominant negative GFP-tagged caveolin-1 or the EGFP control and infected with BPV1 PsVs carrying the DsRed reporter gene (Fig. 3J). The transfected/infected cells were analyzed by flow cytometry to determine the percentage of transfected cells that were infected (i.e., double-positive cells). We observed a substantial decrease in BPV1 infection in cells expressing dominant negative caveolin-1 compared to cells expressing the EGFP control (2.4% versus 13.5%, respectively). Experiments were performed in triplicate, and error bars show the standard deviations. The experiments in Fig. 3G and J were performed using BPV1 PsVs from different viral preparations. The input of virions was sufficient for the infection of approximately 5% of 293 cells shown in Fig. 3G and approximately 14% of 293 cells shown in Fig. 3J. The decrease in infection in cells expressing dominant negative caveolin-1 indicates that caveolin-1 may be important for the infectious viral pathway.

Caveolin-1 knockdown leads to a loss of BPV1 infection. The decrease in infection seen in 293 cells expressing dominant negative caveolin-1 implied a role for caveolin-1 in BPV1 infection. In order to confirm the importance of caveolin-1 for the intracellular trafficking of BPV1, we knocked down expression using shRNA against caveolin-1 (Fig. 4A and B). It was first necessary to determine whether the shRNA was indeed effectively decreasing caveolin-1 expression and whether the caveolin-1 levels within the cell were affected by the presence of our control siRNA directed against luciferase (siRL) (Fig. 4A). The expression levels of both shRNA A and B and siRL were indicated by the coexpression of GFP. 293 cells were plated out and transfected with two versions of the shRNA against caveolin-1, shRNA A and shRNA B. The cells were infected with siRL in a lentiviral vector as our negative control. Forty-eight hours after transfection of shRNA A and B and infection with siRL, the 293 cells were harvested. Western blotting demonstrated that caveolin-1 protein levels were indeed knocked down in 293 cells transfected with shRNA A and

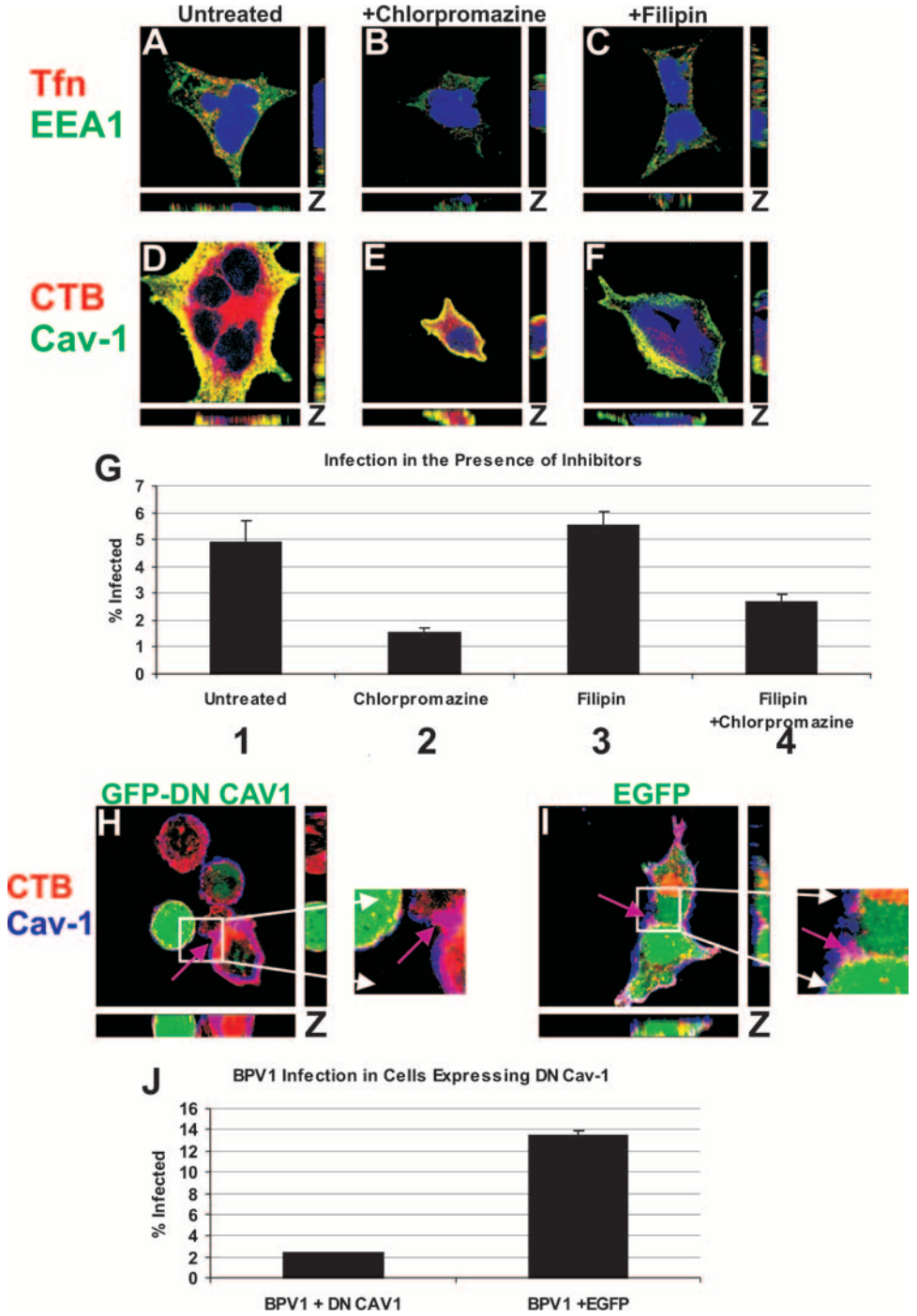

FIG. 3. Cholesterol sequestration by filipin does not affect BPV1 infection, but a dominant negative caveolin-1 mutant inhibits BPV1 infection. (A to F) 293 cells pretreated for 1 h with chlorpromazine (B and E) or filipin (C and F) were allowed to internalize Tfn (A to C, red) or CTB (D to F, red) for 30 min. The cells were stained for EEA1 (A to C, green) or caveolin-1 (Cav-1) (D to F, green), and the nucleus was stained blue using TOPRO-3. In untreated cells, Tfn colocalized with EEA1 (A, yellow) and CTB overlapped with caveolin-1 (D, yellow). Chlorpromazine treatment resulted in a loss of Tfn detection (B) but normal overlap of CTB with caveolin-1 (E, yellow). Filipin treatment did not affect the colocalization of Tfn with EEA1 (C, yellow) but diminished CTB (F). (G) Inhibitor pretreatment of 293 cells with chlorpromazine decreased infection (bars 2 and 4) compared to filipin treatment (bar 3) or untreated cells (bar 1). Flow cytometry was used to measure GFP expression in infected cells. The experiment was performed in triplicates, and the standard deviations are represented by the error bars. (H to J) The effect of transfecting 293 cells with dominant negative GFP-tagged caveolin-1 (GFP-DN CAV1) (H, green) was compared to that of EGFP expression (I, green). (H and I) CTB (red) was added to transfected cells for 30 min, and cells were stained for endogenous caveolin-1 (blue). In cells expressing dominant negative GFP-tagged caveolin-1 (H, green cell), neither CTB nor caveolin-1 was evident, but an untransfected cell showed internalization of CTB and overlap with caveolin-1 (H, purple arrow). In EGFP-transfected cells (I, green), CTB colocalized with caveolin-1 (I, purple arrow). (J) BPV1 infection of 293 cells transfected with dominant negative caveolin-1 (DN CAV1) or EGFP resulted in a loss of BPV1 infection in cells expressing dominant negative caveolin-1. Transfection was determined by GFP expression, and infection was quantitated by the expression of the DsRed reporter within the pseudovirus. At least 10,000 cells were counted, and bars represent the percentages of transfected cells that were infected (i.e., double positives). Error bars show the standard deviations for data from three experiments.

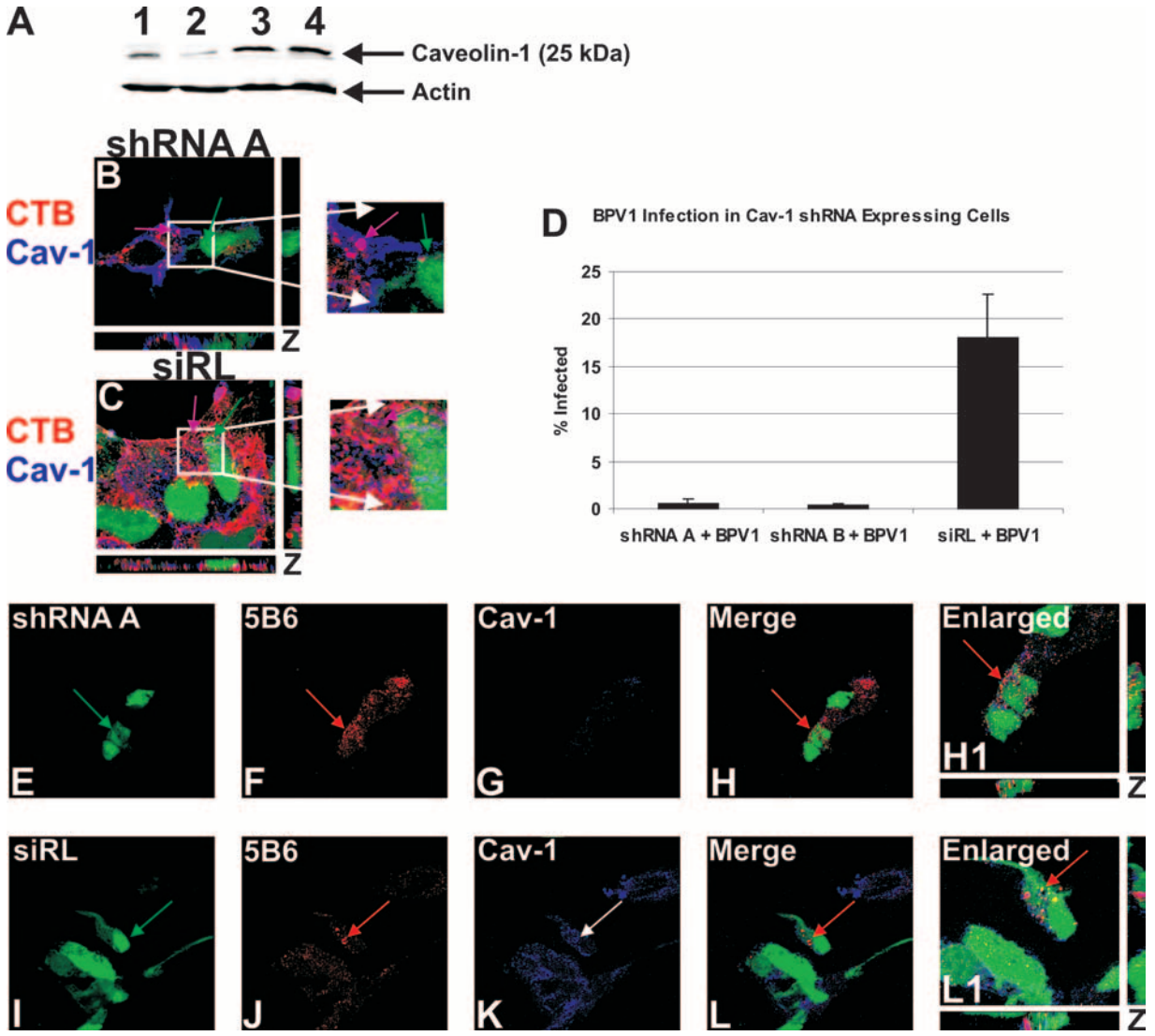

FIG. 4. Knockdown of caveolin-1 expression results in a loss of BPV1 infection despite normal entry. (A) 293 cells were transfected with shRNA A or B against caveolin-1 (lanes 1 and 2, respectively), infected with siRL (lane 3), or untransfected (lane 4). In cells expressing shRNA A and B, protein levels of caveolin-1 were diminished (lanes 1 and 2). The levels of detection of caveolin-1 were comparable in cells expressing siRL (lane 3) and in untransfected cells (lane 4). The actin loading control is shown. (B and C) CTB (red) endocytosis was tested in cells with caveolin-1 (Cav-1) knockdown (shRNA A) (B, green) and cells expressing the siRL (C, green). Endogenous caveolin-1 was stained blue. In cells transfected with shRNA A, caveolin-1 was not detected, and CTB did not bind or enter (B, green arrow). An untransfected cell showed normal CTB trafficking and overlap with caveolin-1 (shRNA A) (B, purple arrow). Cells expressing siRL (C, green arrow) allowed CTB entry, which colocalized with caveolin-1 (C, purple arrow). (D) 293 cells were transfected with shRNA A or B or infected with siRL. Forty-eight hours later, cells were infected with BPV1 PsVs containing the DsRed reporter plasmid. The percentage of transfected cells that were infected was measured by flow cytometry. The knockdown of caveolin-1 led to an almost total loss of infection (shRNA A + BPV1 and shRNA B + BPV1) compared to that of control cells expressing siRL (siRL + BPV1) (D). (E to L) 293 cells were transfected with shRNA A (E to H, green) or infected with siRL (I to L, green) for 48 h and then infected with BPV1 for 30 min. The virus was detected with anti-L1 monoclonal antibody 5B6 (F and J, red), and endogenous caveolin-1 was stained blue (G and K). Cells expressing shRNA A showed virtually no caveolin-1 staining, indicating the effective knockdown of caveolin-1 (G). In the merge and enlarged images, cells lacking caveolin-1 showed the entry of BPV1 PsVs (H and H1, red arrow, merge and enlarged images, respectively). The siRL control cells had normal levels of caveolin-1 (K, blue), and BPV1 endocytosis was evident (L and L1, red arrow, merged and enlarged images, respectively). Enlarged images depict the *z* stack, showing staining in the *x*, *y*, and *z* planes.

B (Fig. 4A, lanes 1 and 2, respectively). Cells that were infected with the siRL control (Fig. 4A, lane 3) showed amounts of caveolin-1 that were approximately equal to those of untransfected cells (Fig. 4A, lane 4). Actin levels are shown to confirm the equal loading of the cellular extracts.

In order to validate the knockdown of caveolin-1, we wanted to determine whether the caveolar ligand CTB was blocked from entering cells expressing shRNA against caveolin-1 (Fig. 4B, green arrow). 293 cells expressing shRNA A or the siRL control (Fig. 4C, green arrow) were allowed to internalize CTB

(red) for 30 min. Endogenous caveolin-1 was stained blue. In GFP-positive cells that were expressing shRNA against caveolin-1 (Fig. 4B, green arrow), we did not detect the presence of caveolin-1 or CTB. An adjacent untransfected cell showed high levels of caveolin-1 colocalizing with CTB at the cell surface, seen as purple (Fig. 4B, purple arrow). The siRL-expressing control cells (Fig. 4C, green arrow) demonstrated CTB internalization that overlapped with caveolin-1 (purple arrow). Our immunofluorescence not only showed the knockdown of caveolin-1 expression but also showed that the internalization of a ligand of caveolin-mediated endocytosis was effectively prevented.

We next wanted to test the effect of caveolin-1 knockdown on BPV1 infection (Fig. 4D). 293 cells were transfected with shRNA A or B against caveolin-1 or infected with the siRL control 48 h prior to infection with BPV1 PsVs containing a DsRed reporter. Cells were harvested after 48 h of infection, and the percentage of GFP-expressing cells that were also DsRed positive (i.e., infected with BPV1 PsV) was determined by flow cytometry. Remarkably, BPV1 infection was essentially blocked in cells deficient of caveolin-1 (Fig. 4D, first and second bars), whereas infection proceeded normally in cells expressing the siRL control (third bar). At least 10,000 cells were collected per sample, and error bars represent the standard deviations from the means of data from three experiments. Our data demonstrate that caveolin-1 is absolutely required for BPV1 infection.

Although we did not see infection in cells lacking caveolin-1, we did not know whether the PsVs were still capable of entering the cell. To explore this possibility, 293 cells grown on coverslips were transfected with shRNA A against caveolin-1 or infected with the lentiviral control, siRL, and infected with BPV1 PsVs for 30 min (Fig. 4E to L). BPV1 was detected with anti-L1 antibody 5B6 (Fig. 4F and J, red), and caveolin-1 was stained blue (Fig. 4G and K). Cells expressing shRNA A (Fig. 4E, green) did not show the presence of caveolin-1, which was seen as a lack of blue in GFP-expressing cells (Fig. 4G). Interestingly, BPV1 particles were still endocytosed into cells lacking caveolin-1 (Fig. 4H and H1, red arrow). In cells expressing the siRL control (Fig. 4I, green), caveolin-1 was detected (Fig. 4K, blue), and BPV1 was again internalized into cells (Fig. 4L and L1, red arrow). These data strongly suggest that caveolin-1 is not needed for the initial entry of BPV1 into cells but is necessary further downstream in the trafficking of the virus.

BPV1 infects cells lacking caveolin-1 at the plasma membrane. Finally, to clarify the role of caveolin-1 in BPV1 infection, 293 cells were transfected with either Myc-tagged WT caveolin-1 or a Myc-tagged caveolin-1 SM (Fig. 5). The SM has been shown to inhibit the movement of caveolin-1-positive vesicles toward the plasma membrane, preventing the internalization of ligands requiring caveola-derived vesicles at the cell surface (32). When the expression of the Myc-tagged constructs was tested in 293 cells, we found high levels of Myc–caveolin-1 expression for both WT and SM caveolin-1 (Fig. 5A, lanes 1 and 2, respectively). There was no Myc band detected in cells transfected with A3M (Fig. 5A, lane 3) or in untransfected cells (Fig. 5A, lane 4).

293 cells grown on coverslips were transfected with WT Myc–caveolin-1 or SM Myc–caveolin-1 to test the effect of the SM on the entry of CTB-594, which utilizes caveolae at the plasma membrane for internalization (Fig. 5B and C, red). The distribution of endogenous caveolin-1 was seen using an antibody against caveolin-1 (green), and WT or SM Myc–caveolin-1 was detected using a 647-labeled anti-Myc antibody (blue) (Fig. 5B and C). The expression of WT caveolin-1 did not alter the binding or entry of CTB, and strong colocalization was seen between CTB, endogenous caveolin-1, and WT Myc–caveolin-1 (Fig. 5B, white arrow) at the cell surface in the *z*-stacked image. We also observed CTB that had trafficked into the cell (Fig. 5B, red arrow). When cells expressed the caveolin-1 SM, we observed a dramatic loss of CTB both at the cell surface and internally (Fig. 5C). The endogenous caveolin-1 (green) and SM caveolin-1 (blue) were seen sequestered away from the plasma membrane (Fig. 5B, aqua arrow).

Having confirmed that the SM was preventing caveolin-1 from reaching the plasma membrane and inhibiting the entry of CTB, we wanted to determine the effect that the mutant would have on BPV1 infection. 293 cells were transfected with WT or SM caveolin-1 and then infected with BPV1 PsVs containing the GFP reporter plasmid (Fig. 5D). After 48 h of infection, the PsVs were harvested for analysis on a flow cytometer. Ten thousand cells were analyzed for each condition, and error bars reflect the standard deviations of data from three experiments. The data implied that BPV1 infection proceeded normally in cells overexpressing the caveolin-1 SM (78.0%) compared to cells overexpressing WT caveolin-1 (86.6%). Percentages given are compared to those of untransfected cells, where the percentage of infection was considered to be 100%. Differences do not appear to be statistically significant due to the margin of error.

To visualize BPV1 infection in cells expressing WT and SM Myc–caveolin-1, 293 cells grown on coverslips were transfected with WT or SM caveolin-1 and infected with BPV1 PsVs for 30 min to determine the entry status of the virus (Fig. 5E and F). Immunofluorescence staining with 647–anti-Myc (Fig. 5E and F, blue) and anti-L1 monoclonal antibody 5B6 (green) showed internalization of BPV1 into cells expressing WT or SM Myc–caveolin-1 (Fig. 5E and F, green arrows). We conclude that the initial entry of BPV1 is independent of caveolin-1, although caveolin-1 appears to be an absolute requirement for BPV1 infection.

DISCUSSION

The intracellular trafficking of ligands has become progressively more complex, particularly in the case of viral entry. While it was previously accepted that most viruses had a strict dependence on a particular route of endocytosis, there is increasing evidence that viruses can utilize multiple means to gain access to the intracellular environment. Previous studies with BPV1 and HPV16 PsVs demonstrated that PV fails to infect cells when the clathrin-mediated pathway but not the caveolar pathway was blocked (12). Many previous studies using dominant negative endocytic inhibitors quantitated total infection levels and did not look specifically at infection in transfected cells; i.e., these experiments could not differentiate levels of viral infection in transfected versus untransfected cells. The accuracy of our studies is based on the use of two-color flow cytometry, allowing us to analyze the differences in

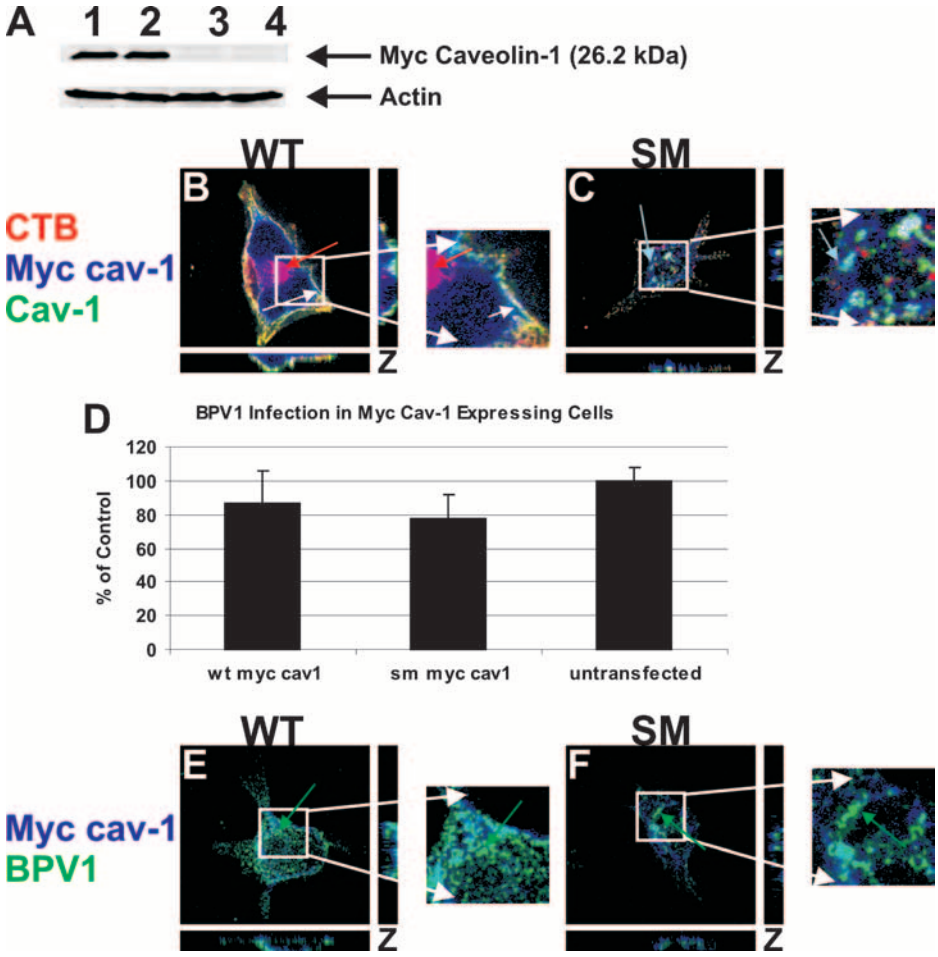

FIG. 5. A caveolin-1 scaffolding mutant does not affect BPV1 infection or entry. 293 cells were transfected with either WT Myc-tagged caveolin-1 or SM Myc-tagged caveolin-1. (A) Western blot analysis showed the overexpression of WT (lane 1) and SM (lane 2) Myc–caveolin-1 constructs. Control cells were transfected with an empty A3M vector (lane 3) or were not transfected (lane 4) and did not show a band for Myc-tagged caveolin-1. (B and C) 293 cells expressing WT caveolin-1 (Cav-1) (B, green) or SM caveolin-1 (C, green) were allowed to internalize CTB (red) for 30 min. A 647-labeled anti-Myc antibody identified transfected cells (blue), and endogenous caveolin-1 was labeled (green). In cells expressing WT caveolin-1, CTB was internalized and colocalized with caveolin-1 and WT caveolin-1, identified by white seen at the plasma membrane (B, white arrow). (C) Expression of SM caveolin-1 led to the sequestration of caveolin-1 away from the plasma membrane and the failure of CTB to bind and enter the cell. The overlap of endogenous caveolin-1 with the SM was seen within the cell (aqua arrow). (D) Infection of 293 cells expressing WT caveolin-1 or the SM of caveolin-1 was the same as infection of untransfected cells. Ten thousand cells were counted by a flow cytometer, and the error bars represent the standard deviations of the means of data from three experiments. (E and F) 293 cells expressing WT or mutant Myc–caveolin-1 constructs were infected with BPV1 PsVs for 30 min. Transfected cells were labeled blue, and BPV1 was detected using 5B6 (green). BPV1 internalized into cells expressing WT caveolin-1 (E, green arrow) and the caveolin-1 SM (F, green arrow). *z*-stacked images show the staining pattern in the *x*, *y*, and *z* planes.

infection in transfected cells expressing the tagged dominant negative protein. This approach has eliminated much of the ambiguity in interpreting the data, as our results are not confounded by differences in transfection efficiencies.

A nonenveloped double-stranded DNA polyomavirus similar in structure to BPV1, JCV, enters into cells by clathrin-mediated endocytosis prior to entering caveolar vesicles, consistent with its later colocalization with the ER marker calregulin (1, 30, 32). Our laboratory has shown evidence of BPV1 localization to the ER by electron microscopy images of BPV1 in the ER (4) and BPV1 colocalization with the ER marker calnexin and ER-resident protein syntaxin 18 (22). Both the viral kinetics of BPV1 (12) and the trafficking to the ER are inconsistent with trafficking that is strictly dependent on the clathrin pathway.

This prompted us to look for evidence suggesting that BPV1 was capable of non-clathrin-dependent entry and trafficking. Using Tfn as a marker for the clathrin-dependent pathway and CTB as a marker for the caveolar pathway, we determined that BPV1 was overlapping with both ligands in a time-dependent manner, showing overlap with Tfn at the earlier time points and cholera toxin later during infection. Importantly, we confirmed that these ligands were trafficking according to their expected routes in 293 cells.

In this paper, we analyzed the colocalization of BPV1 with EEA1, a marker of the early endosome from clathrin-depen-

dent endocytosis (23), and the colocalization of BPV1 with caveolin-1, a scaffolding protein involved in caveola formation and found in caveosomes (27). As with the timing of the overlaps between BPV1 and Tfn and between BPV1 and CTB, the overlap with EEA1 was most prominent at 20 min and diminished by 2 h, whereas BPV1 colocalization with caveolin-1 was nonexistent at 5 min and greatest by 2 h. We did not see an overlap of EEA1 and caveolin-1, suggesting that the vesicles do not interact. This would imply that the colocalizations of BPV1 with EEA1 and caveolin-1 occur in separate intracellular regions.

In order to identify whether caveolin-1 was important for the infectious BPV1 pathway, we wanted to compare the effect of a chemical inhibitor of clathrin-dependent endocytosis to that of an inhibitor of the caveolar pathway. We treated 293 cells with chlorpromazine, which redistributes the adaptor protein responsible for clathrin lattice formation (40), or filipin, a biochemical inhibitor that sequesters cholesterol from lipid rafts on the plasma membrane, disrupting caveola-mediated entry (25). After confirming that chlorpromazine blocked Tfn entry and that filipin was effectively blocking the entry of CTB, we pretreated 293 cells prior to BPV1 infection. Despite our observation by confocal microscopy that BPV1 interacts with caveolin-1, filipin did not negatively affect infection. Pretreatment with both inhibitors did not show a further decrease in infection. We concluded that the sequestration of cholesterol from the plasma membrane did not decrease BPV1 infection; thus, BPV1 entry is not caveolin-1 dependent.

In order to minimize nonspecific inhibition, we used nonchemical methods for altering caveolin-mediated endocytosis. We tested the effect that dominant negative GFP-tagged caveolin-1 would have on the endocytosis of the caveolar ligand CTB and found that dominant negative caveolin-1 effectively prevented its internalization. When we tested the effect that dominant negative caveolin-1 would have on BPV1 infection, we were surprised to find a significant decrease in infection. The failure of filipin to reduce BPV1 infection combined with the substantial decrease in infection using dominant negative caveolin-1 suggested that although caveolin-1 was not needed at the plasma membrane during BPV1 infection, it was playing a role after the initial internalization.

We confirmed the loss of infection seen with dominant negative caveolin-1 by knocking down levels of caveolin-1 using shRNA. Western blot analysis confirmed that we were nearly eliminating caveolin-1 expression in our 293 cells using two different shRNAs against caveolin-1. Immunofluorescence showed that endogenous caveolin-1 was not detected in cells expressing shRNA against caveolin-1 and that CTB internalization in these cells did not occur. When we attempted to infect cells with shRNA-decreased caveolin-1 levels, we saw nearly no BPV1 infection. It is also interesting that shRNA B against caveolin-1 was slightly more effective at decreasing caveolin-1 protein levels than was shRNA A and showed a greater decrease in BPV1 infection. We were curious as to whether BPV1 could enter cells lacking caveolin-1, which would reinforce our hypothesis that caveolin-1 is not needed at early stages of infection (i.e., entry) but is important later. Analysis by confocal microscopy showed that BPV1 PsVs were indeed entering into cells deficient in caveolin-1.

To confirm that although caveolin-1 did not overlap with (and was not required by) BPV1 PsVs at the cell surface but did interact with PsVs postentry, we infected cells expressing a caveolin-1 SM. The caveolin-1 SM redistributes caveolin-1 away from the plasma membrane but does allow for the proper intracellular function and distribution of caveolin-1 in the cytoplasm. The caveolin-1 SM appeared to relocalize caveolin-1 away from the cell surface and prevented CTB binding and entry. Significantly, expression of cells the caveolin-1 SM did not adversely impact BPV1 infection, showing infection levels comparable to those of cells expressing WTcaveolin-1 and to those of untransfected cells, and we observed the colocalization of BPV1 PsVs with the caveolin-1 SM and the Myc-tagged control caveolin-1.

The data described in this paper demonstrate that BPV1 requires clathrin-mediated endocytosis for entry and utilizes the caveolar pathway postentry. The requirement for caveola-mediated endocytosis after initial entry seems to be absolute, as infection was virtually eliminated without caveolin-1. We are exploring the timing of the change in endocytic pathways observed during BPV1 infection and are attempting to determine the mechanism of cross talk between the endosomes and caveolin-1-positive vesicles during BPV1 infection. Several studies have pointed to a Rab5-mediated pathway for the exchange of cargo between the endosome and the caveosome (26, 32). We have obtained siRNA against Rab5, and we will attempt to determine whether Rab5 is playing a role in our system. This is the first demonstration of a PV using both clathrin- and caveolin-1-dependent endocytosis during infection. Our study highlights the capability of viruses to manipulate the trafficking machinery of the cell and provides further insight into the connectedness of two well-known endocytic pathways.

ACKNOWLEDGMENTS

We thank Walter Atwood and William Querbes (Brown University, Providence, RI) for shRNA against caveolin-1 and Myc-tagged wild-type and mutant caveolin-1, and we thank John Schiller and Patricia Day (NCI, NIH, Bethesda, MD) for materials needed for PsV generation. We thank Virginie Bottero (Rosalind Franklin University of Medicine and Science, North Chicago, IL) for the pCSC-SP-PW lentiviral vector and help making the siRNA against luciferase. We thank Rita Levine for her assistance with fluorescence-activated cell sorter analysis at the flow cytometry core at Rosalind Franklin University of Medicine and Science.

The funding for this work was provided by the H. M. Bligh Cancer Research Laboratory of the Rosalind Franklin University of Medicine and Science, NIH/NCI grant K22:CA117971 to P.I.M., and ACS-IL grant 07-34 to P.I.M.

REFERENCES

1. **Belnap, D. M., N. H. Olson, N. M. Cladel, W. W. Newcomb, J. C. Brown, J. W. Kreider, N. D. Christensen, and T. S. Baker.** 1996. Conserved features in papillomavirus and polyomavirus capsids. J. Mol. Biol. **259:**249–263.
2. **Berry, J. M., J. M. Palefsky, and M. L. Welton.** 2004. Anal cancer and its precursors in HIV-positive patients: perspectives and management. Surg. Oncol. Clin. N. Am. **13:**355–373.
3. **Bosch, F. X., X. Castellsague, N. Munoz, S. de Sanjose, A. M. Ghaffari, L. C. Gonzalez, M. Gili, I. Izarzugaza, P. Viladiu, C. Navarro, A. Vergara, N. Ascunce, E. Guerrero, and K. V. Shah.** 1996. Male sexual behavior and human papillomavirus DNA: key risk factors for cervical cancer in Spain. J. Natl. Cancer Inst. **88:**1060–1067.
4. **Bossis, I., R. B. Roden, R. Gambhira, R. Yang, M. Tagaya, P. M. Howley, and P. I. Meneses.** 2005. Interaction of tSNARE syntaxin 18 with the papillomavirus minor capsid protein mediates infection. J. Virol. **79:**6723–6731.
5. **Bousarghin, L., A. Touze, P. Y. Sizaret, and P. Coursaget.** 2003. Human papillomavirus types 16, 31, and 58 use different endocytosis pathways to enter cells. J. Virol. **77:**3846–3850.

6. **Brandenburg, B., L. Y. Lee, M. Lakadamyali, M. J. Rust, X. Zhuang, and J. M. Hogle.** 2007. Imaging poliovirus entry in live cells. PLoS Biol. **5:**e183.
7. **Buck, C. B., D. V. Pastrana, D. R. Lowy, and J. T. Schiller.** 2004. Efficient intracellular assembly of papillomaviral vectors. J. Virol. **78:**751–757.
8. **Campo, M. S.** 2002. Animal models of papillomavirus pathogenesis. Virus Res. **89:**249–261.
9. **Cress, R. D., and E. A. Holly.** 2003. Incidence of anal cancer in California: increased incidence among men in San Francisco, 1973–1999. Prev. Med. **36:**555–560.
10. **Culp, T. D., and N. D. Christensen.** 2004. Kinetics of in vitro adsorption and entry of papillomavirus virions. Virology **319:**152–161.
11. **Damm, E. M., L. Pelkmans, J. Kartenbeck, A. Mezzacasa, T. Kurzchalia, and A. Helenius.** 2005. Clathrin- and caveolin-1-independent endocytosis: entry of simian virus 40 into cells devoid of caveolae. J. Cell Biol. **168:**477–488.
12. **Day, P. M., D. R. Lowy, and J. T. Schiller.** 2003. Papillomaviruses infect cells via a clathrin-dependent pathway. Virology **307:**1–11.
13. **de Sanjose, S., and J. Palefsky.** 2002. Cervical and anal HPV infections in HIV positive women and men. Virus Res. **89:**201–211.
14. **de Villiers, E. M., D. Lavergne, K. McLaren, and E. C. Benton.** 1997. Prevailing papillomavirus types in non-melanoma carcinomas of the skin in renal allograft recipients. Int. J. Cancer **73:**356–361.
15. **de Villiers, E. M., H. Weidauer, H. Otto, and H. zur Hausen.** 1985. Papillomavirus DNA in human tongue carcinomas. Int. J. Cancer **36:**575–578.
16. **Fothergill, T., and N. A. McMillan.** 2006. Papillomavirus virus-like particles activate the PI3-kinase pathway via alpha-6 beta-4 integrin upon binding. Virology **352:**319–328.
17. **Goldenthal, K. L., K. Hedman, J. W. Chen, J. T. August, P. Vihko, I. Pastan, and M. C. Willingham.** 1988. Pre-lysosomal divergence of alpha 2-macroglobulin and transferrin: a kinetic study using a monoclonal antibody against a lysosomal membrane glycoprotein (LAMP-1). J. Histochem. Cytochem. **36:**391–400.
18. **Hagmann, J., and P. H. Fishman.** 1982. Detergent extraction of cholera toxin and gangliosides from cultured cells and isolated membranes. Biochim. Biophys. Acta **720:**181–187.
19. **Hanover, J. A., L. Beguinot, M. C. Willingham, and I. H. Pastan.** 1985. Transit of receptors for epidermal growth factor and transferrin through clathrin-coated pits. Analysis of the kinetics of receptor entry. J. Biol. Chem. **260:**15938–15945.
20. **Hindmarsh, P. L., and L. A. Laimins.** 2007. Mechanisms regulating expression of the HPV 31 L1 and L2 capsid proteins and pseudovirion entry. Virol. J. **4:**19.
21. **Krauzewicz, N., J. Stokrova, C. Jenkins, M. Elliott, C. F. Higgins, and B. E. Griffin.** 2000. Virus-like gene transfer into cells mediated by polyoma virus pseudocapsids. Gene Ther. **7:**2122–2131.
22. **Laniosz, V., K. C. Nguyen, and P. I. Meneses.** 2007. Bovine papillomavirus type 1 infection is mediated by SNARE syntaxin 18. J. Virol. **81:**7435–7448.
23. **Mu, F. T., J. M. Callaghan, O. Steele-Mortimer, H. Stenmark, R. G. Parton, P. L. Campbell, J. McCluskey, J. P. Yeo, E. P. Tock, and B. H. Toh.** 1995. EEA1, an early endosome-associated protein. EEA1 is a conserved alpha-helical peripheral membrane protein flanked by cysteine "fingers" and contains a calmodulin-binding IQ motif. J. Biol. Chem. **270:**13503–13511.
24. **Muller, M., L. Gissmann, R. J. Cristiano, X. Y. Sun, I. H. Frazer, A. B. Jenson, A. Alonso, H. Zentgraf, and J. Zhou.** 1995. Papillomavirus capsid binding and uptake by cells from different tissues and species. J. Virol. **69:**948–954.
25. **Orlandi, P. A., and P. H. Fishman.** 1998. Filipin-dependent inhibition of cholera toxin: evidence for toxin internalization and activation through caveolae-like domains. J. Cell Biol. **141:**905–915.
26. **Pelkmans, L., T. Burli, M. Zerial, and A. Helenius.** 2004. Caveolin-stabilized membrane domains as multifunctional transport and sorting devices in endocytic membrane traffic. Cell **118:**767–780.
27. **Pelkmans, L., and A. Helenius.** 2002. Endocytosis via caveolae. Traffic **3:**311–320.
28. **Pelkmans, L., and A. Helenius.** 2003. Insider information: what viruses tell us about endocytosis. Curr. Opin. Cell Biol. **15:**414–422.
29. **Pelkmans, L., J. Kartenbeck, and A. Helenius.** 2001. Caveolar endocytosis of simian virus 40 reveals a new two-step vesicular-transport pathway to the ER. Nat. Cell Biol. **3:**473–483.
30. **Pho, M. T., A. Ashok, and W. J. Atwood.** 2000. JC virus enters human glial cells by clathrin-dependent receptor-mediated endocytosis. J. Virol. **74:**2288–2292.
31. **Querbes, W., A. Benmerah, D. Tosoni, P. P. Di Fiore, and W. J. Atwood.** 2004. A JC virus-induced signal is required for infection of glial cells by a clathrin- and eps15-dependent pathway. J. Virol. **78:**250–256.
32. **Querbes, W., B. A. O'Hara, G. Williams, and W. J. Atwood.** 2006. Invasion of host cells by JC virus identifies a novel role for caveolae in endosomal sorting of noncaveolar ligands. J. Virol. **80:**9402–9413.
33. **Roden, R. B., H. L. Greenstone, R. Kirnbauer, F. P. Booy, J. Jessie, D. R. Lowy, and J. T. Schiller.** 1996. In vitro generation and type-specific neutralization of a human papillomavirus type 16 virion pseudotype. J. Virol. **70:**5875–5883.
34. **Roden, R. B., R. Kirnbauer, A. B. Jenson, D. R. Lowy, and J. T. Schiller.** 1994. Interaction of papillomaviruses with the cell surface. J. Virol. **68:**7260–7266.
35. **Rommel, O., J. Dillner, C. Fligge, C. Bergsdorf, X. Wang, H. C. Selinka, and M. Sapp.** 2005. Heparan sulfate proteoglycans interact exclusively with conformationally intact HPV L1 assemblies: basis for a virus-like particle ELISA. J. Med. Virol. **75:**114–121.
36. **Sharma, D. K., A. Choudhury, R. D. Singh, C. L. Wheatley, D. L. Marks, and R. E. Pagano.** 2003. Glycosphingolipids internalized via caveolar-related endocytosis rapidly merge with the clathrin pathway in early endosomes and form microdomains for recycling. J. Biol. Chem. **278:**7564–7572.
37. **Sieczkarski, S. B., and G. R. Whittaker.** 2002. Dissecting virus entry via endocytosis. J. Gen. Virol. **83:**1535–1545.
38. **Sieczkarski, S. B., and G. R. Whittaker.** 2002. Influenza virus can enter and infect cells in the absence of clathrin-mediated endocytosis. J. Virol. **76:**10455–10464.
39. **Smith, J. L., S. K. Campos, and M. A. Ozbun.** 2007. Human papillomavirus type 31 uses a caveolin 1- and dynamin 2-mediated entry pathway for infection of human keratinocytes. J. Virol. **81:**9922–9931.
40. **Wang, L. H., K. G. Rothberg, and R. G. Anderson.** 1993. Mis-assembly of clathrin lattices on endosomes reveals a regulatory switch for coated pit formation. J. Cell Biol. **123:**1107–1117.
41. **Zheng, Z. M., and C. C. Baker.** 2006. Papillomavirus genome structure, expression, and posttranscriptional regulation. Front. Biosci. **11:**2286–2302.